Subcell Treatment of Sloped Interfaces between Debye Materials in the FDTD Method

*Kenan Tekbas

Amasya University, Technology Faculty, Department of Electrical and Electronics Engineering, Amasya TURKEY

ORCID:0000-0002-0678-9001

Abstract

This paper presents the application of the subcell technique for the treatment of sloped interface in finite-difference time-domain method. The technique is based on the averaging of permittivities in each cell crossed by the material interface. The frequency-dependent behaviour of materials was characterized using one-pole Debye model. The numerical experiment was conducted on the two-dimensional space.

Key Words: FDTD, finite-difference time-domain, sloped interface

Özet

Bu makale, sonlu farklı zaman alanı yönteminde eğimli arayüzün tedavisi için alt hücre tekniğinin uygulanması sunmaktadır. Teknik, malzeme ara yüzü ile geçen her bir hücredeki geçirgenliklerin ortalamasına dayanmaktadır. Malzemelerin frekansa bağımlı davranışı, tek kutuplu Debye modeli kullanılarak karakterize edildi. Sayısal deney iki boyutlu uzayda gerçekleştirildi.

Anahtar Kelimeler: FDTD, sonlu-ayrık zaman-alanı, eğimli arayüz

1. Introduction

The finite-difference time-domain (FDTD) method is widely used to analyse and understand the electromagnetic waves interaction problems (Taflove and Hagness, 2007). The method provides to solve very complex problems where it is not possible to achieve a solution with analytical studies. However, the method suffers from the staircase error when modelling sloped or curved surfaces due to inaccurate approximation of geometry in a regularly spaced orthogonal FDTD lattice. In early studies, (Jurgen et al., 1992) introduced a contour path model for dealing with the curved surfaces of materials in the rectangular FDTD grid. The model improved the accuracy to model arbitrary complex geometry but shows the late time instabilities. Then, (Day and Mittra, 1997) studied a locally conformal algorithm for accurately modelling curved metallic objects. The results showed that the algorithm is more accurate than obtained by using stair-casing approach. (Kaneda et al., 1997) also presented a different technique that calculates the effective permittivities for arbitrarily shaped dielectric interfaces. Later, (Yu and Mittra, 2001) proposed to treat curved dielectric objects by overcoming the instability but sacrificing accuracy. Recently, (Zhao and Hao, 2007) addressed two-dimensional modelling of cylindrical waveguides, where the frequency-dependent permittivity was characterised by the Drude model. However, the method requires a complex fourth-order discretisation procedure. (Argyropoulos et al, 2009) investigated both lossless and lossy electromagnetic clocks. Nevertheless, the method deals with a high order differential equation which makes its usage impractical. All the techniques outlined above tackle very specific problems and geometrical shapes. In this paper, we demonstrate the application of the subcell technique in (Tekbas et al, 2017) for approximation of the sloped surface between two frequency-dependent media characterized by the Debye model in a two-dimensional FDTD space. The technique does not downgrade the second-order accuracy of the standard FDTD method due to maintaining the uniform mesh structure of the standard FDTD method. Moreover, the orthogonal structure of the standard FDTD method is not disrupted, which makes the implementation of the algorithm straightforward.

2. FDTD Subcell Formula for the Treatment of Sloped Interface

The FDTD method solves space and time derivatives of Maxwell's curl equations in the time domain using the central difference approximations. Maxwell's curl equations in material independent form are

$$\nabla \times \mathbf{E} = -\frac{\partial \mathbf{B}}{\partial t} \tag{1}$$

$$\nabla \times \mathbf{H} = \frac{\partial \mathbf{D}}{\partial t} \tag{2}$$

where **E, H, D** and **B** are the electric field, magnetic field, electric flux density and magnetic flux density, respectively. The constitutive relationship for non-magnetic media is $\mathbf{B} = \mu_0 \mathbf{H}$ where μ_0 is the permeability of vacuum and for one-pole Debye media is, in frequency domain

$$\mathbf{D} = \varepsilon_0 \left[\varepsilon_\infty - \frac{\varepsilon_\infty - \varepsilon_S}{1 + j\omega\tau} - j\frac{\sigma}{\omega\varepsilon_0} \right] \mathbf{E} \tag{3}$$

where ε_0, ε_∞ and ε_S are the vacuum, the optical and the static relative permittivities respectively, τ is the relaxation time and σ is the conductivity. Eq. (3) can be rewritten as

$$(j\omega)^2\tau\mathbf{D} + j\omega\mathbf{D} = (j\omega)^2\varepsilon_0\varepsilon_\infty\tau\mathbf{E} + j\omega(\varepsilon_0\varepsilon_S + \sigma\tau)\mathbf{E} + \sigma\mathbf{E} \tag{4}$$

Taking into account the time dependence of $\exp(j\omega t)$, Eq.(4) transforms into time domain as

$$\tau\frac{d^2\mathbf{D}}{dt^2} + \frac{d\mathbf{D}}{dt} = \varepsilon_0\varepsilon_\infty\tau\frac{d^2\mathbf{E}}{dt^2} + (\varepsilon_0\varepsilon_S + \sigma\tau)\frac{d\mathbf{E}}{dt} + \sigma\mathbf{E}. \tag{5}$$

The discretization of time derivatives and the averaging of the last term over time in Eq.(4) leads to

$$\begin{aligned}
E_u^{n+1} &= \frac{4\varepsilon_0\varepsilon_\infty\tau + 2(\varepsilon_0\varepsilon_S + \sigma\tau)\Delta t - \sigma(\Delta t)^2}{2\varepsilon_0\varepsilon_\infty\tau + 2(\varepsilon_0\varepsilon_S + \sigma\tau)\Delta t + \sigma(\Delta t)^2} E_u^n \\
&\quad - \frac{2\varepsilon_0\varepsilon_\infty\tau}{2\varepsilon_0\varepsilon_\infty\tau + 2(\varepsilon_0\varepsilon_S + \sigma\tau)\Delta t + \sigma(\Delta t)^2} E_u^{n-1} \\
&\quad + \frac{2\Delta t + 2\tau}{2\varepsilon_0\varepsilon_\infty\tau + 2(\varepsilon_0\varepsilon_S + \sigma\tau)\Delta t + \sigma(\Delta t)^2} D_u^{n+1}
\end{aligned} \tag{6}$$

$$-\frac{2\Delta t + 4\tau}{2\varepsilon_0\varepsilon_\infty\tau + 2(\varepsilon_0\varepsilon_S + \sigma\tau)\Delta t + \sigma(\Delta t)^2}D_u^n$$

$$+\frac{2\tau}{2\varepsilon_0\varepsilon_\infty\tau + 2(\varepsilon_0\varepsilon_S + \sigma\tau)\Delta t + \sigma(\Delta t)^2}D_u^{n-1}$$

where *u=x, y* and *z*. Let us consider transverse magnetic mode radiation respect to *z* direction, Eq(1) and Eq(2) lead to three coupled partial differential equations

$$\frac{\partial H_x}{\partial t} = -\frac{1}{\mu_0}\frac{\partial E_z}{\partial y} \tag{7}$$

$$\frac{\partial H_y}{\partial t} = \frac{1}{\mu_0}\frac{\partial E_z}{\partial x} \tag{8}$$

$$\frac{\partial D_z}{\partial t} = \frac{\partial H_y}{\partial x} - \frac{\partial H_x}{\partial y} \tag{9}$$

The temporal and spatial discretisation of of (7), (8) and (9) lead to

$$H_x^{n+1/2}(i,j+1/2) = H_x^{n-1/2}(i,j+1/2) - \frac{\Delta t}{\mu_0\Delta y}[E_z^n(i,j+1) - E_z^n(i,j)], \tag{10}$$

$$H_y^{n+1/2}(i+1/2,j) = H_y^{n-1/2}(i+1/2,j) + \frac{\Delta t}{\mu_0\Delta x}[E_z^n(i+1,j) - E_z^n(i,j)], \tag{11}$$

$$D_z^{n+1}(i,j) = D_z^n(i,j) + \frac{\Delta t}{\Delta x}\left[H_y^{n+1/2}(i+1/2,j) - H_y^{n+1/2}(i-1/2,j)\right]$$
$$-\frac{\Delta t}{\Delta y}\left[H_x^{n+1/2}(i,j+1/2) - H_x^{n+1/2}(i,j-1/2)\right]. \tag{12}$$

where *n* is the time step number, Δt is the temporal discretisation, Δx and Δy are special discretisation in *x* and *y* directions, *i* and *j* are the indices of the field component in the FDTD lattice, respectively (Taflove and Hagness, 2007). D_z is collocated with E_z. Let us consider the oblique surface between two Debye media, as depicted in Fig.1.
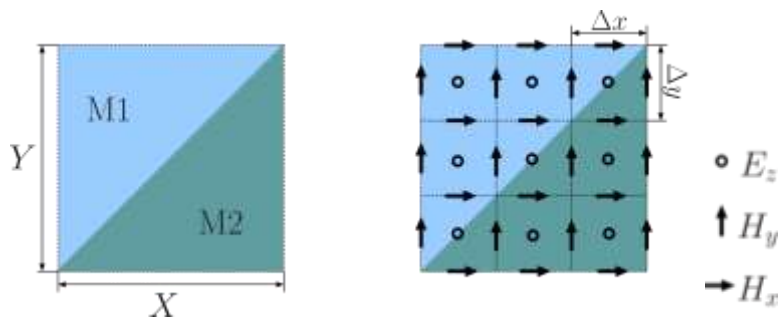
Figure. 1 The sloped interface between two Debye media in two-dimensional space.

When the FDTD method is applied to the problem space, there are two possible ways to model the sloped interface between two media, either by filling the intersect cell with Debye medium 1 (M1) or with Debye medium 2 (M2) as illustrated in Fig.2.
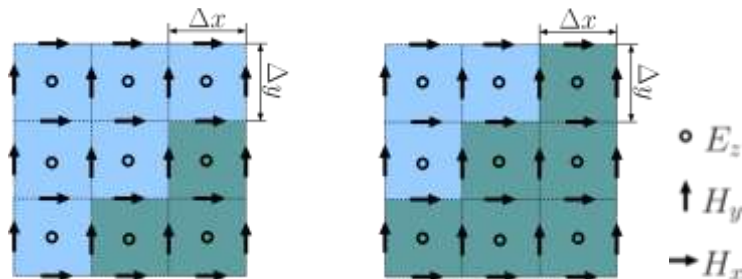

Figure. 2 A $\Delta x \times \Delta y$ FDTD cell is filled with one of Debye media.

The approach in Fig.2 may introduce a large numerical error depending on the dielectric properties of media if the resolution of spatial sampling is not small enough. To alleviate this error, one may consider applying the subcell technique in the intersect cell where it can allow for the contribution of both Debye media in the cell. The subcell technique for Debye media was given in details in (Tekbas et al, 2017). The component of E_z can be advanced using

$$E_z^{n+1} = \gamma_1 \left[\Psi_z^{n+1} + \gamma_2 E_z^n - \gamma_3 E_z^{n-1} - \gamma_4 D_{z_1}^n + \gamma_5 D_{z_1}^{n-1} - \gamma_6 D_{z_2}^n + \gamma_7 D_{z_2}^{n-1} \right] \qquad (13)$$

where

$$\gamma_1 = \left(\frac{2\varepsilon_0\varepsilon_{\infty_1}\tau_1 + 2(\varepsilon_0\varepsilon_{S_1} + \sigma_1\tau_1)\Delta t + \sigma_1(\Delta t)^2}{2(\Delta t + \tau_1)} s_1 \right.$$

$$\left. + \frac{2\varepsilon_0\varepsilon_{\infty_2}\tau_2 + 2(\varepsilon_0\varepsilon_{S_2} + \sigma_2\tau_2)\Delta t + \sigma_2(\Delta t)^2}{2(\Delta t + \tau_2)} s_2 \right)^{-1},$$

$$\gamma_2 = \frac{4\varepsilon_0\varepsilon_{\infty_1}\tau_1 + 2(\varepsilon_0\varepsilon_{S_1} + \sigma_1\tau_1)\Delta t - \sigma_1(\Delta t)^2}{2(\Delta t + \tau_1)} s_1$$

$$+ \frac{4\varepsilon_0\varepsilon_{\infty_2}\tau_2 + 2(\varepsilon_0\varepsilon_{S_2} + \sigma_2\tau_2)\Delta t - \sigma_2(\Delta t)^2}{2(\Delta t + \tau_2)} s_2,$$

$$\gamma_3 = \frac{\varepsilon_0\varepsilon_{\infty_1}\tau_1}{\Delta t + \tau_1} s_1 + \frac{\varepsilon_0\varepsilon_{\infty_2}\tau_2}{\Delta t + \tau_2} s_2, \qquad \gamma_4 = \frac{\Delta t + 2\tau_1}{\Delta t + \tau_1} s_1, \qquad \gamma_5 = \frac{\tau_1}{\Delta t + \tau_1} s_1,$$

$$\gamma_6 = \frac{\Delta t + 2\tau_2}{\Delta t + \tau_2} s_2, \qquad \gamma_7 = \frac{\tau_2}{\Delta t + \tau_2} s_2$$

ε_{∞_1}, ε_{S_1}, σ_1 and τ_1 are the media parameters of *M1* and ε_{∞_2}, ε_{S_2}, σ_2 and τ_2 are the media parameters of *M2*. s_1 and s_2 are partial surfaces, D_{z_1} and D_{z_2} are the flux densities of *M1* and *M2* respectively. The auxiliary quantity Ψ_z in (13) is calculated as

$$\Psi_z^{n+1}(i,j) = \Psi_z^n(i,j) - \frac{\Delta t}{\Delta x} \left[H_y^{n+1/2}(i+1/2,j) - H_y^{n+1/2}(i-1/2,j) \right]$$

$$- \frac{\Delta t}{\Delta y} \left[H_x^{n+1/2}(i,j+1/2) - H_x^{n+1/2}(i,j-1/2) \right] \qquad (14)$$

Therefore, (10) can be used to update H_x, (11) to update H_y, (14) to update Ψ_z, (13) to update E_z and (6) to update D_z for each medium i.e. the iteration is complete.
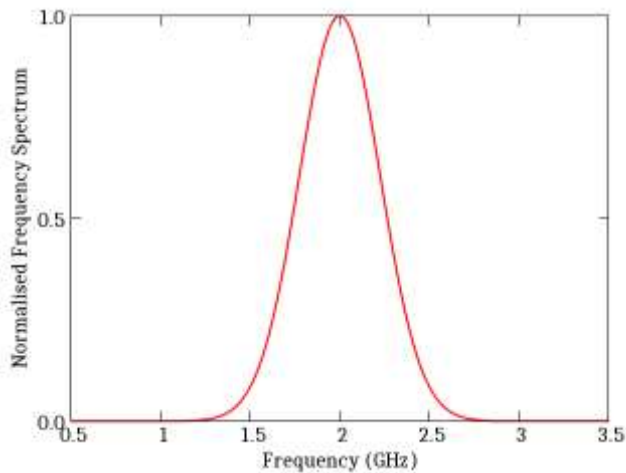
3. Numerical Experiment

The incident wave for the simulation was a modulated Gaussian pulse given by

$$g(t) = 100 \, e^{-\left(\frac{t-5\varsigma}{\varsigma}\right)^2} cos(2\pi f_c t)$$

where ς and f_c are the bandwidth and the carrier frequency, respectively. Fig.3. shows the Gaussian pulse, when ς and f_c were set 0.1 ns and 2.0 GHz, respectively.
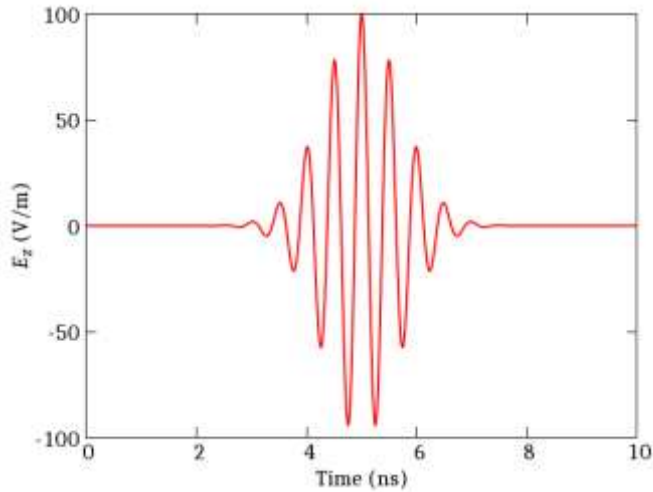
a)   Time domain

b)   Frequency domain

Figure 3. The incident pulse in time and frequency domain.

The pulse was introduced into the FDTD space using Huygens' method which is commonly known as the total-field/scattered-field method (Taflove and Hagness, 2007). The FDTD steps were set $\Delta x=\Delta y=0.1$ mm and $\Delta t=0.17$ ns for the fine mesh reference and $\Delta x=\Delta y=1$ mm and $\Delta t=1.7$ ns for the coarse mesh calculations. The total FDTD cell size was 600×600 and 60×60 for the fine mesh and coarse mesh, respectively. As an example, a $X \times Y=3 \times 3$ mm square shown in Fig.1 was placed in vacuum. The media properties of *M1* and *M2* are given in Table I.

Table I. Media parameters

Media	ε_S	ε_∞	σ (S/m)	τ(ps)
M1	47.9	29.9	0.540	43.6
M2	14.2	7.36	0.104	34.1

The E_z was observed in the scattered field region at each simulation. In Fig.4, "fine mesh-1" denotes the results obtained by setting $\Delta x=\Delta y=0.1$ mm and filling the intersect cell with *M1* whereas "fine mesh-2" with *M2.* In the same manner, "coarse mesh-1" denotes the results obtained by setting $\Delta x=\Delta y=1$ mm and filling the intersect cell with *M1* whereas "coarse mesh-2" with *M2.* Fig 4. shows that the coarse mesh results give substantially different from the fine grid references with $\Delta x =\Delta y=0.1$ mm. However, the result with the subcell treatment with $\Delta x=\Delta y=1$ mm match the fine mesh references. In all calculations, the instability was not observed.
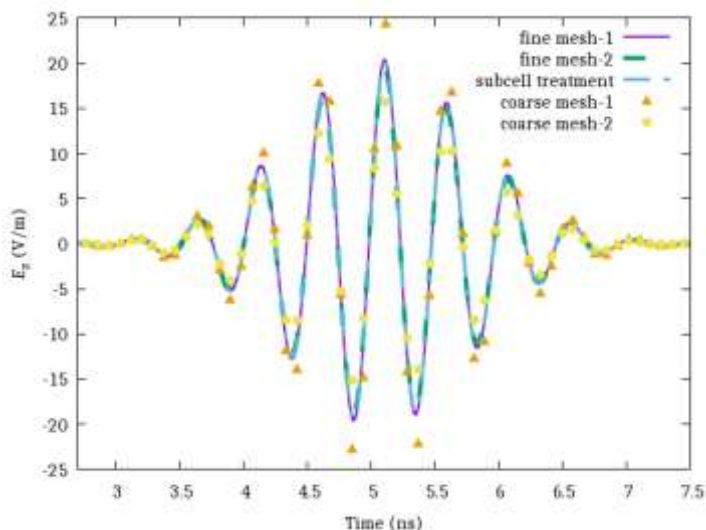

Figure 4. Observation of E_z in the scattered-field region.

4. Conclusion

This paper shows that the subcell treatment reduces the error caused by the incorrect media distribution in the cell. However, it does not fully mitigate the error of staircase approximation in FDTD grid. The method can be applied to the transverse electric mode by treating the normal component as in (Maloney and Smith, 1992) and to other mathematical models of materials such as Lorentz and Drude as well. Furthermore, the method can be incorporated into a more sophisticated approach using tensors (Nadobny, 2003).

5. Acknowledgement

6. Conflicts of interest

The authors declare that there are no potential conflicts of interest relevant to this article.

7. References

C. Argyropoulos, Y. Zhao, and Y. Hao. "A radially-dependent dispersive finite-difference time-domain method for the evaluation of electromagnetic cloaks," in IEEE Trans. Antennas Propag., 57(5):1432–1441, May 2009.

J. G. Maloney and G. S. Smith. "The efficient modeling of thin material sheets in the finite-difference time-domain (FDTD) method, " IEEE Trans. Antennas Propag., 40(3):323–330, Mar 1992.

J. Nadobny, D. Sullivan, W. Wlodarczyk, P. Deuflhard and P. Wust, "A 3-D tensor FDTD-formulation for treatment of sloped interfaces in electrically inhomogeneous media," in IEEE Trans. Antennas Propag., vol. 51, no. 8, pp. 1760-1770, Aug. 2003.

K. Tekbas, F. Costen, J. Bérenger, R. Himeno and H. Yokota, "Subcell Modeling of Frequency-Dependent Thin Layers in the FDTD Method," in IEEE Trans. Antennas Propag.,, vol. 65, no. 1, pp. 278-286, Jan. 2017

N. Kaneda, B. Houshmand, and T. Itoh. "FDTD analysis of dielectric resonators with curved surfaces," IEEE Trans. Microw. Theory. Tech., 45(9):1645–1649, September 1997.

S. Dey and R. Mittra. "A locally conformal finite-difference time-domain (FDTD) algorithm for modeling three-dimensional perfectly conducting objects," IEEE Microw. Wirel. Compon. Lett., 7(9):273–275, Sep 1997.

Taflove, A. & Hagness, S. C. (2005), Computational electrodynamics: the finite-difference time-domain method , Artech House , Norwood

T. G. Jurgens, A. Taflove, K. Umashankar, and T. G. Moore. "Finite-difference time-domain modeling of curved surfaces, " IEEE Trans. Antennas Propag., 40(4):357–366, Apr 1992.

W. Yu and R. Mittra. "A conformal finite difference time domain technique for modeling curved dielectric surfaces, " IEEE Microw. Compon. Lett., 11(1):25–27, Jan 2001.

Y. Zhao and Y. Hao. "Finite-difference time-domain study of guided modes in nano-plasmonic waveguides, " IEEE Trans. Antennas Propag., 55(11):3070–3077, Nov 2007.